Biochemical and Biophysical Research Communications 490 (2017) 182–188

Contents lists available at ScienceDirect

Biochemical and Biophysical Research Communications

journal homepage: www.elsevier.com/locate/ybbrc

GSK3 inhibitor AR-A014418 promotes osteogenic differentiation of human adipose-derived stem cells via ERK and mTORC2/Akt signaling pathway

Min Zhang [a], Ping Zhang [a], Yunsong Liu [a], Yongsheng Zhou [a, b, *]

[a] Department of Prosthodontics, Peking University School and Hospital of Stomatology, Beijing 100081, China
[b] National Engineering Lab for Digital and Material Technology of Stomatology, Beijing Key Laboratory of Digital Stomatology, Peking University School and Hospital of Stomatology, Beijing 100081, China

ARTICLE INFO

Article history:
Received 27 May 2017
Accepted 7 June 2017
Available online 8 June 2017

Keywords:
AR-A014418
Human adipose-derived stem cells (hASCs)
Osteogenic differentiation
GSK3
ERK1/2
RICTOR

ABSTRACT

Small molecule-based bone tissue engineering is emerging as a promising strategy for bone defects restoration. In this study, we intended to identify the roles and mechanisms of AR-A014418, a highly selective inhibitor of GSK3, on the osteogenic differentiation. We found that AR-A014418 exhibited a dose-dependent effect on osteogenic differentiation of human adipose-derived stem cells (hASCs). hASCs treated with AR-A014418 showed higher activity of ERK and mTORC2/Akt signaling. Administration of ERK inhibitor U0126 or knockdown of RICTOR by siRNA attenuated AR-A014418 induced osteogenic differentiation of hASCs. Our results suggested that AR-A014418 significantly promoted osteogenic potential of hASCs partially by the activation of ERK and mTORC2/Akt signaling pathway, and might be used for bone tissue engineering as an osteo-inductive factor.

1. Introduction

Oral bone defects, resulting from systemic disease, congenital defects, tumor resection, inflammation or trauma, remains a great challenge for clinician. Autologous bone grafting is regarded as the "gold standard" for repairing such bone defects. Nevertheless, disadvantages such as donor site morbidity, protracted surgery and limited available volume, hinder its clinical application [1,2]. By combination of seed cells, bioactive carriers and growth factors, bone tissue engineering (BTE) is emerging as a promising strategy for regenerative medicine. Mesenchymal stem cells (MSCs) are widely applied for BTE due to their self-renewal and multiple differentiation potential [3,4]. Human adipose-derived stem cells (hASCs) is becoming a very promising method for BTE, taking advantage of their properties of abundant source, easy accessibility, and high yield efficiency [5]. Recently, several small molecules have been discovered with osteogenic activity through various signaling mechanisms [6–8]. Moreover, small molecules are non-immunogenic, more stable, easy to be synthetic and cost-effective [9]. Therefore, small molecule seems to be an attractive alternative for growth factor to amplify the stem cells population or direct their osteogenic differentiation.

Glycogen synthase kinase-3 (GSK3) belongs to serine-threonine protein kinase family. It participates in many pathophysiological courses such as cell proliferation, stem cell pluripotency and lineage commitment, embryogenesis and oncogenesis. GSK3 is an essential component of a variety of key signaling pathways such as Wnt/beta-catenin, BMP/Smad, mTOR and NF-κB [10–12]. It has been well documented that the lineage differentiation of MSCs is tightly regulated by the aforementioned signaling pathways. Therefore, small molecules targeting GSK3 may provide new therapeutic strategies for MSCs-based bone regeneration. However, conclusions of previous studies dealing with the effects of GSK3 on bone regeneration are controversial [13,14]. Moreover, mechanisms by which GSK3 regulated bone regeneration mostly related to BMP/Smad and Wnt/beta-catenin signaling in the previous studies [15]. Data is still scarce of the crosstalk between GSK3 and other signaling pathways in bone formation. Taken together, more researches are needed to discover new GSK3 inhibitors with powerful osteo-inductive potential and to unravel the intricate molecular

* Corresponding author. Department of Prosthodontics, Peking University School and Hospital of Stomatology, 22 Zhongguancun South Avenue, Haidian District, Beijing 100081, China.
E-mail addresses: miwryz@126.com (M. Zhang), zhangping332@bjmu.edu.cn (P. Zhang), kqliuyunsong@163.com (Y. Liu), kqzhouysh@hsc.pku.edu.cn (Y. Zhou).

http://dx.doi.org/10.1016/j.bbrc.2017.06.018
0006-291X/

mechanisms of GSK3 in MSCs lineage differentiation.

AR-A014418 is reported as a highly selective inhibitor of GSK3, which inhibits GSK3 activity in an ATP-competitive manner and does not inhibit CDK2, CDK5 or 26 other kinases [16]. In this study, we explored the roles of AR-A014418 on osteogenic differentiation of hASCs, and investigated the underlying molecular mechanisms.

2. Methods

2.1. Cell culture and osteogenic differentiation

Primary hASCs were obtained from ScienCell (Carlsbad, CA, USA). The experiments were repeated three times with third passage cells from three independent donors. Cells were cultured in proliferation media (PM) containing DMEM containing 10% fetal bovine serum, 100U/ml penicillin G and 100 mg/mL streptomycin. For osteogenic differentiation, cells were cultured in osteogenic media (OM) containing 100 nM dexamethasone (Sigma-Aldrich, St. Louis, MO, USA), 0.2 mM ascorbic acid (Sigma-Aldrich), and 10 mM β-glycerophosphate (Sigma-Aldrich).

2.2. Cell proliferation assay

AR-A014418 and U0126 were obtained from Sigma-Aldrich. The cell proliferative ability was detected with the Cell Counting Kit-8 assay kit (Dojindo, Kumamoto, Japan). At each time point, the supernatant of each group was discarded. Then cells were incubated with DMEM media added with CCK-8 reagent for 2 h at 37 °C, according to the manufacture's protocol. The absorbance value was measured at 450 nm using a microplate reader (ELX808, BioTek).

2.3. Alkaline phosphatase (ALP) activity analysis

Cells were cultured in osteogenic media for 7 days in 12-well plates. ALP staining was performed using a BCIP/NBT staining kit (CWBIO, Beijing, China) according to the manufacture's protocol. For ALP activity quantification, cells were washed thrice with PBS and lysed with 1% TritonX-100 (Sigma-Aldrich) for 10 min on ice. The cells were harvested and centrifuged at 12,000 rpm for 30 min at 4 °C. Protein concentration of the collected supernatants was measured using a BCA protein assay kit (Pierce Thermo Scientific, MA, USA). The ALP quantification assay was detected using an ALP activity kit (Nanjing Jiancheng Bioengineering Institute, Nanjing, China). Relative ALP activity was compared with that in the controls and normalized by the total protein concentration.

2.4. Alizarin Red S staining and quantification

After cultured with OM for 14 days, cells were fixed with 4% paraformaldehyde, and rinsed three times with distilled water. Then cells were incubated with 2% Alizarin Red S staining solution (pH 4.2, Sigma-Aldrich). For quantification of mineralization, the staining was incubated in 100 mM cetylpyridinium chloride (Sigma-Aldrich) for 1 h. The optical density value was measured at 562 nm and normalized by the total protein concentration detected in a duplicate plate.

2.5. RNA extraction, reverse transcription, and quantitative real-time PCR

Total RNA was extracted with TRIzol reagent (Invitrogen, Carlsbad, CA, USA). Reverse transcription was conducted with a PrimeScript RT Reagent Kit (Takara, Tokyo, Japan). Quantitative real-time PCR assays were conducted using SYBR Green PCR Master Mix as described on an ABI 7500 real-time PCR system (Applied Biosystems, CA, USA). Glyceraldehyde 3-phosphate dehydrogenase (*GAPDH*) was used as internal control for normalization. The primers used are listed in Table 1.

2.6. Western blotting

Cells were lysed with radioimmunoprecipitation assay (RIPA) buffer containing protease inhibitor cocktail (Roche). Lysates were centrifuged at 12000 rpm at 4 °C for 30 min. Protein concentrations of the supernatants were measured using a BCA protein assay kit (Thermo Scientific). Aliquots (30 μg) of each sample were subjected to 10% SDS PAGE and then transferred to polyvinylidene difluoride membrane (Millipore). The membranes were blocked with 5% skim milk for 1 h to avoid non-specific reactivity. Then the blots were incubated with indicated primary antibodies overnight at 4 °C. Then the blots were incubated with peroxidase-linked secondary antibodies at room temperature for 1 h. The membranes were detected using an ECL kit (CWBIO) to visualize the bound antibodies. The antibodies used were anti-β-Catenin, anti-GAPDH; anti-phospho-GSK3α/β (Ser21/9), anti-GSK3α/β (Ser21/9), anti-phospho-ERK1/2 (Thr202), anti-ERK1/2, anti-RICTOR, anti-p-Akt (Ser473), anti-Akt (Cell Signaling, Danvers, MA, USA). GAPDH was used as internal control.

2.7. Bone formation in vivo

Cells were cultured to 100% confluence *in vitro*, resuspended and incubated with β-TCP (Bicon, Boston, MA, USA). The nude mice was transplanted with two groups of cells on the dorsal subcutaneous space: hASC/Dimethyl Sulphoxide (DMSO), hASC/AR-A014418 (10 μM) in two sites. Transplants were collected at 4 weeks, fixed in 4% paraformaldehyde and then decalcified in 10% EDTA (PH 7.4) for 10 days. Following dehydration, the samples were embedded in paraffin. Sections (5 μm) were used for the histological staining, including haematoxylin and eosin (H&E), Masson's trichrome stain, and immunohistochemical (IHC) staining for Osteocalcin (OCN) (Abcam). All animal experiments in this study were approved by Peking University Biomedical Ethics Committee Experimental Animal Ethics Branch.

2.8. Small interfering RNA

siRNAs targeting *RICTOR* and negative control siRNA (NC-FAM) were obtained from Genepharma. siRNA sequences were: si*RICTOR*-1: AAGCAGCCTTGAACTGTTTA-A; si*RICTOR*-2: AAACTTGTGAAGAATCGTATC. Cells at 70%–80% confluence were transfected with 5 nM of siRNA using Lipofectamine RNAi-MAX (Invitrogen) and cultured for the indicated days.

2.9. Statistical analysis

Statistical calculation were conducted using the GraphPad Prism software (San Diego, CA, USA). All values were shown as the

Table 1
Sequences primers of selected genes designed for real-time PCR.

Genes	Forward primer	Reverse primer
GAPDH	TGTTCGACAGTCAGCCGCAT	CGCCCAATACGACCAAATCCGT
RUNX2	ACCACAAGTGCGGTGCAAAC	ACTGCTTGCAGCCTTAAATGACTCT
ALP	TAAGGACATCGCCTACCAGCTC	TCTTCCAGGTGTCAACGAGGT
OCN	CACCATGAGAGCCCTCACACTC	CCTGCTTGGACACAAAGGCTGC
BSP	TGCCAGAGGAAGCAATCACCA	GTGGCCTGTACTTAAAGACCCCA
CCND1	GCTGCGAAGTGGAAACCATC	CCTCCTTCTGCACACATTTGAA
MYC	ATTTGGGGACACTTCCCCGC	GGGAGGCTGCTGGTTTTCCA

mean ± standard deviation (SD) of three independent experiments. The Student's *t*-tests were used for comparison between two groups. One-way ANOVA was used for multiple-group condition. Statistical significance was authentic when P values < 0.05.

3. Results

3.1. Effect of AR-A014418 on proliferation of hASCs

hASCs were cultured under proliferation media with or without AR-A014418 at a series of concentrations. CCK8 assay was used to analyze hASCs proliferation. As shown in Fig. 1, AR-A014418 inhibited hASCs proliferation in a dose-dependent manner. No significant interference was shown in the cell viability with a concentration less than or equal to 10 μM. However, the inhibition occurred at the concentration up to 20 μM–50 μM. Thus, AR-A014418 concentrations no more than 10 μM were used for the remaining experiments.

3.2. AR-A014418 treatment enhanced osteogenic differentiation of hASCs

To evaluate the biological effect of AR-A014418 on osteogenic differentiation *in vitro*, hASCs were differentiated into osteoblast in the presence of osteogenic inducer, and various concentrations of AR-A014418 (1 μM, 5 μM or 10 μM). As shown in Fig. 2A–2C, AR-A014418 treatment significantly promoted osteogenic differentiation *in vitro* in a dose-dependent manner compared with untreated group. ALP activity was upregulated significantly in cells treated with AR-A014418 after osteogenic induction for 7 days (Fig. 2A). Moreover, Alizarin Red S staining and quantification showed that extracellular matrix mineralization was also increased by AR-A014418 treatment after osteogenic induction for 14 days (Fig. 2B). The maximal and significant effect was observed at concentration of 10 μM. AR-A014418 significantly upregulated the mRNA expression level of *RUNX2*, *ALP*, *OCN* and *BSP* (Fig. 2C). To further confirm the effect of AR-A014418 on osteogenesis, we next explored whether AR-A014418 improved hASCs mediated osteogenesis *in vivo*. hASCs pre-treated with DMSO or AR-A014418 (10 μM) for 3 days were loaded in β-TCP scaffolds and implanted in nude mice for 4 weeks. As shown in Fig. 2D (left), H&E staining revealed that compared with control group, cells pre-treated with AR-A014418 formed more eosinophilic bone-like structures with fewer cells in the extracellular matrix (ECM). Masson's trichrome staining showed that AR-A014418 treated group generated more collagen (Fig. 2D middle). Moreover, immunohistochemical (IHC) staining showed that more strong expression of OCN (an osteogenic marker) was found in AR-A014418 treated group compared to DMSO group (Fig. 2D right). Quantitative measurements showed that the bone formation area was increased significantly in AR-A014418 treated group (Fig. 2E). Collectively, these results indicated that AR-A014418 is a positive regulator of osteogenic differentiation.

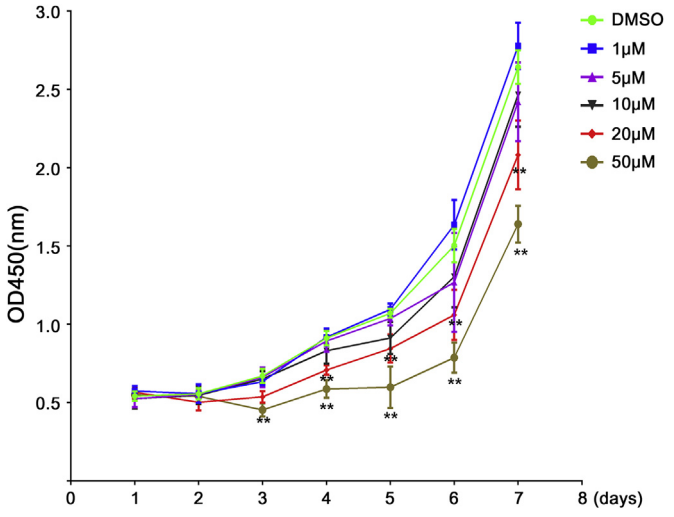

Fig. 1. Effect of AR-A014418 on cell viability of hASCs. hASCs were cultured in proliferation media with or without AR-A014418. DMSO was used as control group. No significant changes were found in the proliferative capacity of hASCs cultured with 1, 5, or 10 μM AR-A014418 compared with control group. The concentration of 20 μM began to slow cell proliferation at day 4. At the concentration of 50 μM, hASCs proliferation was slowed at day 3. Values are expressed as the mean ± S.D (n = 3). $^{**}P < 0.01$.

3.3. AR-A014418 activated the Wnt/beta-catenin, ERK and mTORC2/Akt signaling pathway in hASCs

To investigate the molecular mechanisms of AR-A014418 in the process of osteogenic differentiation, we detected the effect of AR-A014418 on the activation of Wnt/beta-catenin, ERK and mTORC2/Akt signaling pathways. As seen in Fig. 3A, treatment with AR-A014418 upregulated β-catenin expression in hASCs. The expression level of phosphorylation GSK-3α (Ser21) and GSK3β (Ser9) increased along with a decrease in total GSK3 expression. Meanwhile, the mRNA expression level of *CCND1* and *MYC* was increased in AR-A014418 treated group (Fig. 3B). Moreover, the phosphorylation level of ERK1/2 was significantly increased by AR-A014418 treatment (Fig. 3C). In addition, we found that AR-A014418 upregulated the protein expression of RICTOR. RICTOR is a core component of mTORC2/Akt signaling pathway. The phosphorylation level of Akt was also increased in AR-A014418 treated hASCs (Fig. 3D).

3.4. ERK and mTORC2/Akt signaling pathway were involved in AR-A014418 regulated osteogenesis

Next, we intended to detect the role of ERK and mTORC2/Akt signaling pathways in AR-A014418 regulated osteogenesis. First, we treated hASCs with ERK1/2 inhibitor U0126. We found that U0126 significantly reduced the mineralization ability of AR-A014418 treated cells (Fig. 4A). *RICTOR* siRNA were used to blocking mTORC2/Akt signaling activity. RICTOR expression was significantly reduced as detected by western blotting (Fig. 4B). Alizarin Red S staining and quantification revealed that the increased osteogenic differentiation ability induced by AR-A014418 treatment was effectively reversed by *RICTOR* siRNA (Fig. 4C). Furthermore, *RUNX2*, *ALP* and *OCN* mRNA expression also decreased significantly in RICTOR deficiency cells (Fig. 4D). Taken together, these results suggested that ERK and mTORC2/Akt signaling pathways were involved in the process of AR-A014418 induced osteogenic differentiation.

4. Discussion

Taking advantages of its own properties, small molecule inhibitors of GSK3 are emerging as a promising strategy for bone tissue engineering. In the present study, we focused on the effects and mechanisms of AR-A014418, a GSK3 specific inhibitor, on the osteogenic differentiation of hASCs. First, we intended to find out the optimal concentration range of AR-A014418 on the viability of hASCs. CCK8 assay demonstrated that AR-A014418 inhibited hASCs proliferation at a concentration of 20 μM up to 50 μM, whereas less than or equal to 10 μM had no effects on the cell viability. On the basis of the results, a concentration range from 1 μM to 10 μM was

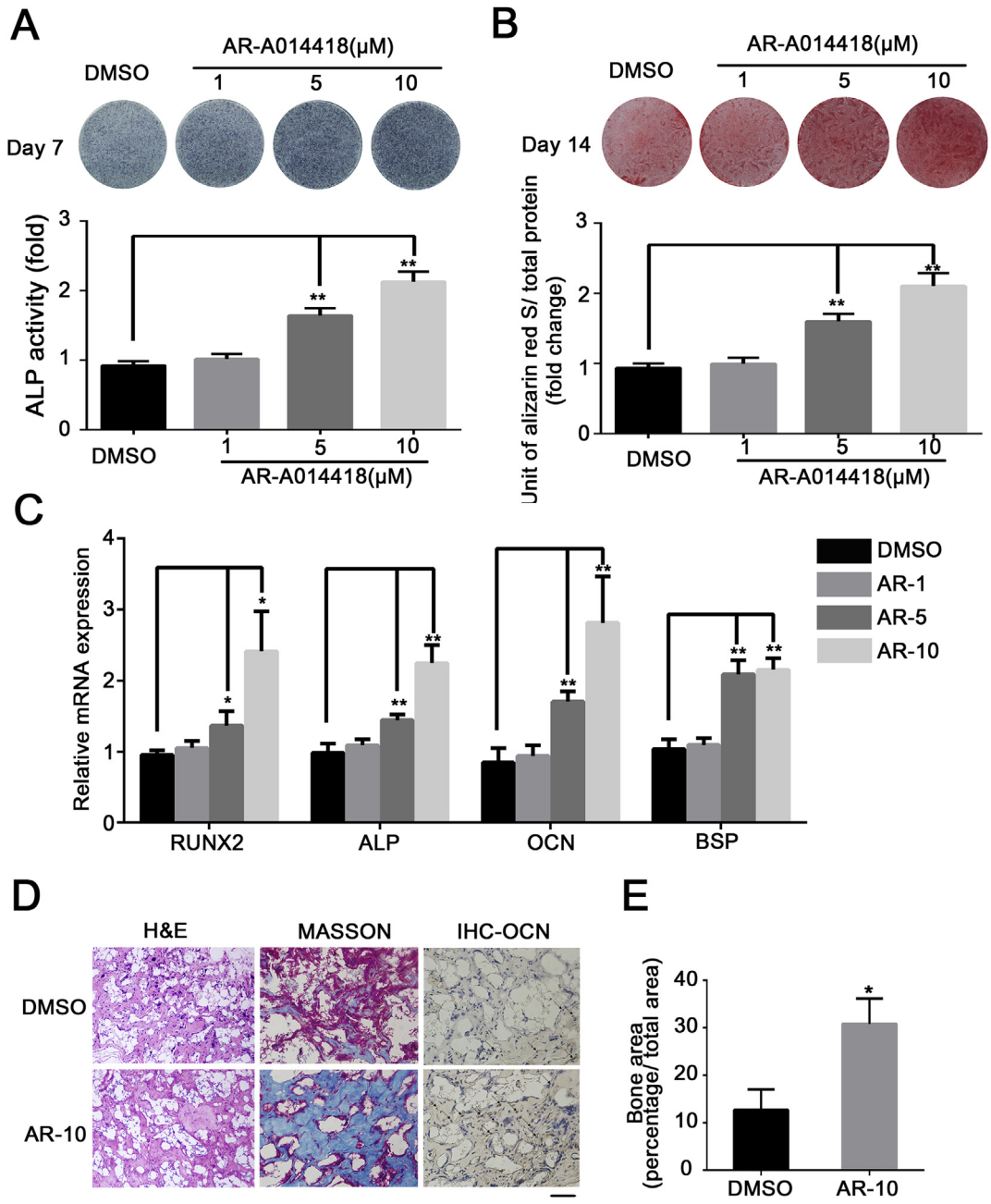

Fig. 2. AR-A014418 treatment enhanced osteogenic differentiation of hASCs. (A) ALP staining and quantitation. AR-A014418 treatment enhanced the ALP activity of hASCs. (B) Alizarin Red S staining and quantitation. AR-A014418 at 5 μM and 10 μM accelerated mineralization of hASCs. (C) AR-A014418 treatment promoted the expression levels of *RUNX2*, *ALP*, *OCN* and *BSP* in hASCs, as assessed by RT-qPCR. *RUNX2* and *ALP* were detected at day 7. *OCN* and *BSP* were detected at day 14 after osteogenic differentiation. (D) AR-A014418 treatment enhanced hASCs-induced osteogenesis *in vivo*. (Left) H&E staining showed that more eosinophilic bone-like structures were formed in AR-A014418 treated group. (Middle) Masson's trichrome staining. Newly generated collagen was stained blue-green. (Right) IHC staining for OCN. AR-A014418 treated group exhibited more positive staining (black arrows). (E) Quantitative measurements of bone-like tissues. Values are expressed as the mean ± S.D (n = 3).Scale bar represents 50 μm $^{*}P < 0.05$ and $^{**}P < 0.01$. AR: AR-A014418.

selected for the remaining tests.

hASCs treated with AR-A014418 at the concentration of 5 μM and 10 μM presented enhanced ALP activity and extracellular matrix mineralization. The mRNA expression levels of *RUNX2*, *ALP*, *OCN* and *BSP* were upregulated in a dose-dependent manner. Moreover, we evaluated the role of AR-A014418 on the osteogenic differentiation of hASCs *in vivo* by subcutaneous transplantation model in nude mice. A concentration of 10 μM was used for the *in vivo* assay. Our findings suggested that AR-A014418 treatment induced a significant increase in bone-like tissue formation, collagen deposition, and protein expression of OCN. These results indicated that AR-A014418 could promote the osteogenic differentiation of hASCs and might serve as a powerful osteogenic inducer in bone tissue engineering.

The activity of GSK3 is down regulated by serine residues phosphorylation (S21 for GSK3α and S9 for GSK3β) and up regulated by tyrosine residues phosphorylation (Tyr 279 for GSK3α and Tyr216 for GSK3β) [17]. In our study, we found that AR-A014418 increased the phosphorylation levels of serine residues in hASCs, resulting in the decrease of total GSK3 activity. GSK3 is a key

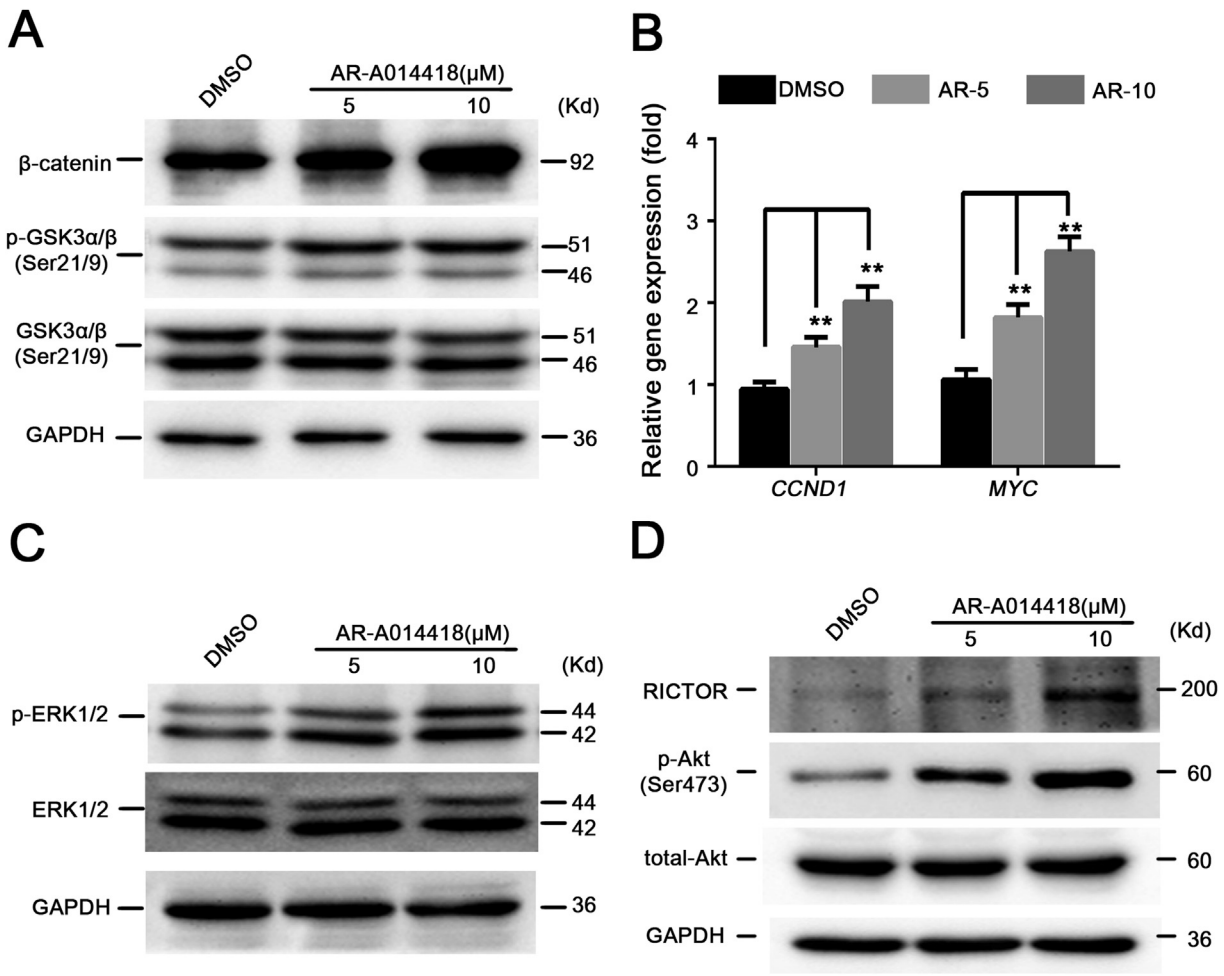

Fig. 3. AR-A014418 activated the Wnt/beta-catenin, ERK and mTORC2/Akt signaling pathway in hASCs. Cells were cultured in proliferation media with the indicated concentration of AR-A014418 for 48 h. (A) Western blotting analysis of β-catenin, p-GSK3α/β (Ser21/9) and GSK3α/β (Ser21/9). GAPDH was used as internal control. (B) Relative mRNA expression of Wnt/beta-catenin target gene *CCND1* and *MYC* measured by RT-qPCR. (C) Western blotting analysis of p-ERK1/2 and ERK1/2. GAPDH was used as internal control. (D) Western blotting analysis of RICTOR, p-Akt (Ser473), Akt. GAPDH was used as internal control. Values are expressed as the mean ± S.D (n = 3). $^{**}P < 0.01$.

component of Wnt/beta-catenin signaling. GSK3 inhibition results in β-catenin aggregation in cytoplasm and translocation to nucleus [18]. We found that AR-A014418 treatment led to an increase in β-catenin protein level and mRNA expression level of canonical Wnt signaling target genes, *CCND1* and *MYC*. These result indicated that the activation of Wnt/beta-catenin might contribute to AR-A014418 induced osteogenesis.

We observed an increased activation of ERK signaling in hASCs treated with AR-A014418. Previous work of our group have indicated that activation of ERK signaling promotes the osteogenic differentiation of hASCs [19]. Treatment with U0126 could reverse the enhanced mineralization ability induced by AR-A014418. ERK phosphorylated GSK3β at the T43 residue, leading to GSK3β suppression [20]. ERK activation was also important for regulation of GSK3β activity in MSCs [21]. Here, our results showed that inhibition of GSK3 activated ERK signaling, and the increased ERK signaling activity contributed to AR-A014418 promoted osteogenesis. These results suggested a new regulatory loop between ERK1/2 and GSK3 in the osteogenic differentiation of hASCs.

Rictor/mTORC2 have been established to play an essential role in osteogenic differentiation of MSCs. Rictor-deficient MSCs showed reduced osteogenic differentiation capacity alone with lowered activity of the mTORC2-Akt (Ser473) signaling pathway. Deletion of *Rictor* in genetically modified mice resulted in impaired bone formation with thinner cortical bone [22,23]. In our study, the protein level of RICTOR and the phosphorylation level of Akt were upregulated in hASCs treated with AR-A014418. Furthermore, knockdown of RICTOR attenuated the upregulation effect of AR-A014418 on osteogenic differentiation of hASCs. We also observed that silencing of RICTOR decreased the osteogenic capacity of hASCs treated with DMSO, which was consistent with the previous studies in murine marrow-derived MSCs [22]. These data indicated that RICTOR was involved in the AR-A014418 promoted osteogenic differentiation of hASCs. Recent studies demonstrated that RICTOR is a substrate of GSK3β. Chen et al. [24] identified that GSK3β phosphorylated the RICTOR at serine 1235, resulting in an inhibition on the binding of Akt to mTORC2. Koo, J et al. [25] reported that RICTOR is degraded through an FBXW7-mediated ubiquitination/proteasome mechanism and this process requires phosphorylation of RICTOR at threonine 1695 by GSK3. Our results suggested that there might be a new regulatory loop of GSK3, Akt, and RICTOR during hASCs osteogenic differentiation.

In summary, we identified GSK3 inhibitor AR-A014418 could promote the osteogenic differentiation of hASCs *in vitro* and enhance bone formation *in vivo*. The activation of ERK and mTORC2/Akt signaling pathway contributed to AR-A014418 induced osteogenesis of hASCs, unraveling the new regulatory loop (GSK3/ERK, GSK3/mTORC2-Akt) in the osteogenic

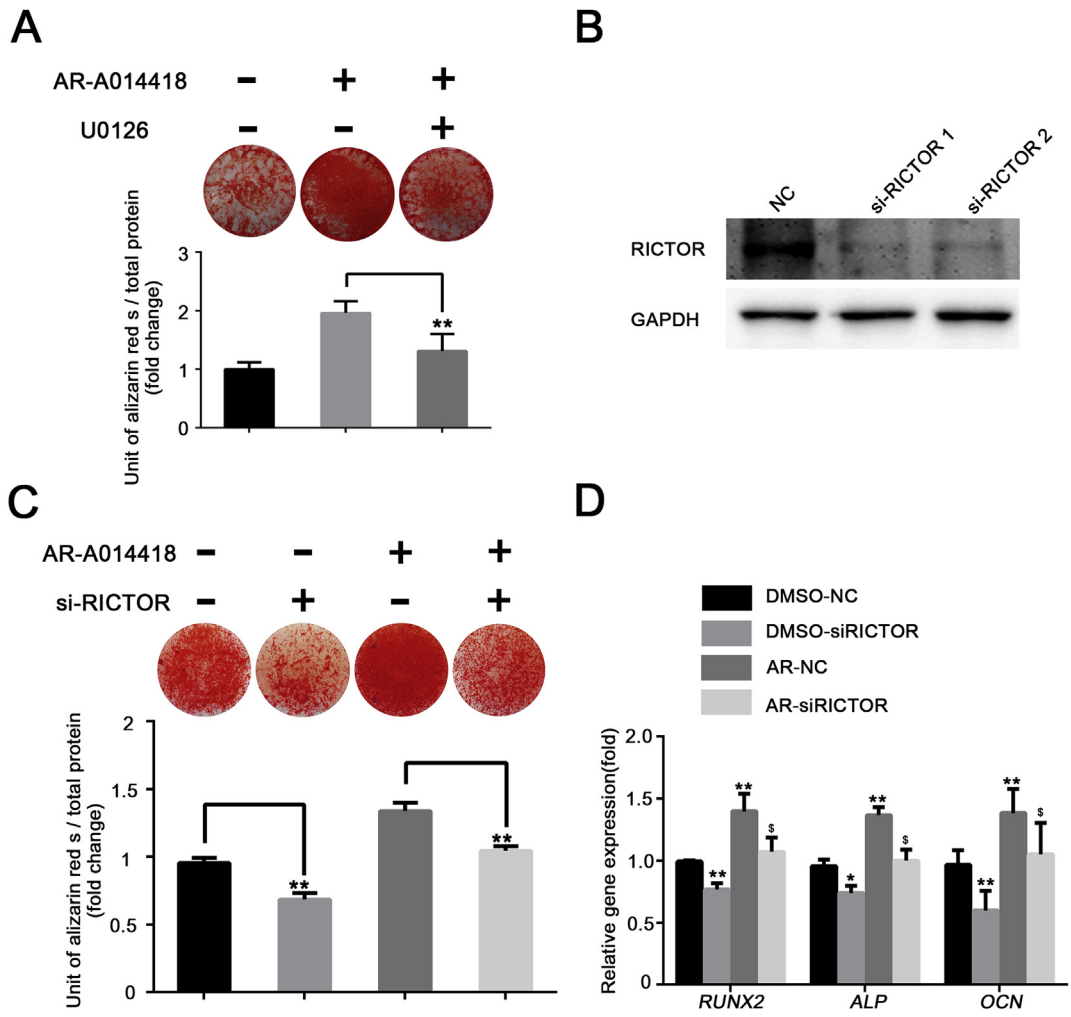

Fig. 4. ERK and RICTOR were involved in AR-A014418 regulated osteogenesis. (A) U0126 inhibited the promoting effect of AR-A014418 on the osteogenic differentiation of hASCs. hASCs were cultured in osteogenic induction medium with or without AR-A014418 (10 μM), or U0126 (10 μM) for 14 days. Alizarin Red S staining and quantification were used to detect the mineralization ability of hASCs. (B) Knockdown of RICTOR was validated by western blotting. Cells treated with proliferation media were harvested after transfection with siRNA of RICTOR for 48 h. A mixture of siRICTOR-1 and siRICTOR-2 was used for the following experiments in Fig. 4C–4D. (C) Alizarin Red staining and quantification. AR-A014418-induced osteoblastic mineralization was attenuated after functional disruption of RICTOR in hASCs. (D) Relative mRNA expression of RUNX2, ALP, and OCN. RUNX2 and ALP were detected at day 7. OCN was detected at day 14 after osteogenic differentiation. AR-A014418 (10 μM) was used for the study. Values are expressed as the mean ± S.D (n = 3). *P < 0.05 compared to DMSO-NC, **P < 0.01 compared to DMSO-NC, and $ P < 0.05 compared to AR-NC. NC: negative control; AR: AR-A014418.

differentiation of hASCs. Based on these results, AR-A014418 may serve as a novel osteogenic inducer in bone tissue engineering.

Conflict of interest

The authors declare no conflicts of interest.

Acknowledgements

This work was supported by the National Natural Science Foundation of China [grant number 81570953, 81500822]; the Project for Culturing Leading Talents in Scientific and Technological Innovation of Beijing [grant number Z171100001117169]; the Grant of Peking University School of Stomatology for Talented Young Investigators [grant number PKUSS20140109].

Transparency document

Transparency document related to this article can be found online at http://dx.doi.org/10.1016/j.bbrc.2017.06.018.

References

[1] M. Yoshioka, K. Tanimoto, Y. Tanne, et al., Bone regeneration in artificial jaw cleft by use of carbonated hydroxyapatite particles and mesenchymal stem cells derived from iliac bone, Int. J. Dent. 2012 (2012) 352510.
[2] C. Liu, X. Tan, J. Luo, et al., Reconstruction of beagle hemi-mandibular defects with allogenic mandibular scaffolds and autologous mesenchymal stem cells, PLOS One 9 (2014) e105733.
[3] W.L. Grayson, B.A. Bunnell, E. Martin, et al., Stromal cells and stem cells in clinical bone regeneration, Nat. Rev. Endocrinol. 11 (2015) 140–150.
[4] H. Saeed, M. Ahsan, Z. Saleem, et al., Mesenchymal stem cells (MSCs) as skeletal therapeutics - an update, J. Biomed. Sci. 23 (2016) 41.
[5] R. Dai, Z. Wang, R. Samanipour, et al., Adipose-derived stem cells for tissue engineering and regenerative medicine applications, Stem Cells Int. 2016 (2016) 6737345.
[6] B.H. Chung, J.D. Kim, C.K. Kim, et al., Icariin stimulates angiogenesis by activating the MEK/ERK- and PI3K/Akt/eNOS-dependent signal pathways in human endothelial cells, Biochem. Biophys. Res. Commun. 376 (2008) 404–408.
[7] J. Pagkalos, J.M. Cha, Y. Kang, et al., Simvastatin induces osteogenic differentiation of murine embryonic stem cells, J. Bone Min. Res. 25 (2010) 2470–2478.
[8] E.J. Carbone, T. Jiang, C. Nelson, et al., Small molecule delivery through nanofibrous scaffolds for musculoskeletal regenerative engineering, Nanomedicine-UK 10 (2014) 1691–1699.
[9] K.W. Lo, K.M. Ashe, H.M. Kan, et al., The role of small molecules in musculoskeletal regeneration, Regen. Med. 7 (2012) 535–549.

[10] K.P. Hoeflich, J. Luo, E.A. Rubie, et al., Requirement for glycogen synthase kinase-3beta in cell survival and NF-kappaB activation, Nature 406 (2000) 86–90.
[11] F. Vigneron, S.P. Dos, S. Lemoine, et al., GSK-3beta at the crossroads in the signalling of heart preconditioning: implication of mTOR and Wnt pathways, Cardiovasc. Res. 90 (2011) 49–56.
[12] M.A. Schoeman, M.J. Moester, A.E. Oostlander, et al., Inhibition of GSK3beta stimulates BMP signaling and decreases SOST expression which results in enhanced osteoblast differentiation, J. Cell. Biochem. 116 (2015) 2938–2946.
[13] N.H. Kulkarni, J.E. Onyia, Q. Zeng, et al., Orally bioavailable GSK-3alpha/beta dual inhibitor increases markers of cellular differentiation in vitro and bone mass in vivo, J. Bone Min. Res. 21 (2006) 910–920.
[14] J.E. Huh, R. Ko, H.J. Jung, et al., Glycogen synthase kinase 3beta promotes osteogenic differentiation of murine adipose-derived stromal cells, PLOS One 8 (2013) e54551.
[15] E. Biver, C. Thouverey, D. Magne, et al., Crosstalk between tyrosine kinase receptors, GSK3 and BMP2 signaling during osteoblastic differentiation of human mesenchymal stem cells, Mol. Cell. Endocrinol. 382 (2014) 120–130.
[16] R. Bhat, Y. Xue, S. Berg, et al., Structural insights and biological effects of glycogen synthase kinase 3-specific inhibitor AR-A014418, J. Biol. Chem. 278 (2003) 45937–45945.
[17] E. Beurel, S.F. Grieco, R.S. Jope, Glycogen synthase kinase-3 (GSK3): regulation, actions, and diseases, Pharmacol. Ther. 148 (2015) 114–131.
[18] L.H. Hoeppner, F.J. Secreto, J.J. Westendorf, Wnt signaling as a therapeutic target for bone diseases, Expert Opin. Ther. Targets 13 (2009) 485–496.
[19] M. Zhang, P. Zhang, Y. Liu, et al., RSPO3-LGR4 regulates osteogenic differentiation of human adipose-derived stem cells via ERK/FGF signalling, Sci. Rep. 7 (2017) 42841.
[20] Q. Ding, W. Xia, J.C. Liu, et al., Erk associates with and primes GSK-3beta for its inactivation resulting in upregulation of beta-catenin, Mol. Cell. 19 (2005) 159–170.
[21] J.H. Shim, M.B. Greenblatt, W. Zou, et al., Schnurri-3 regulates ERK downstream of WNT signaling in osteoblasts, J. Clin. Invest. 123 (2013) 4010–4022.
[22] B. Sen, Z. Xie, N. Case, et al., mTORC2 regulates mechanically induced cytoskeletal reorganization and lineage selection in marrow-derived mesenchymal stem cells, J. Bone Min. Res. 29 (2014) 78–89.
[23] J. Chen, N. Holguin, Y. Shi, et al., mTORC2 signaling promotes skeletal growth and bone formation in mice, J. Bone Min. Res. 30 (2015) 369–378.
[24] C.H. Chen, T. Shaikenov, T.R. Peterson, et al., ER stress inhibits mTORC2 and Akt signaling through GSK-3beta-mediated phosphorylation of rictor, Sci. Signal 4 (2011) ra10.
[25] J. Koo, X. Wu, Z. Mao, et al., Rictor undergoes glycogen synthase kinase 3 (GSK3)-dependent, FBXW7-mediated ubiquitination and proteasomal degradation, J. Biol. Chem. 290 (2015) 14120–14129.